PAPER • OPEN ACCESS

Simulation study for the IceCube IceTop enhancement with a scintillator array

View the article online for updates and enhancements.

IOP ebooks™

Bringing you innovative digital publishing with leading voices to create your essential collection of books in STEM research.

Start exploring the collection - download the first chapter of every title for free.

Simulation study for the IceCube IceTop enhancement with a scintillator array

Agnieszka Leszczyńska[1] for the IceCube-Gen2 Collaboration

[1]Institut of Nuclear Physics, KIT - Karlsruhe Institute of Technology, Germany

E-mail: `agnieszka.leszczynska@kit.edu`

Abstract. The IceTop upgrade foresees the deployment of a scintillation-detector array placed within the IceTop footprint. This will improve the current measurements of cosmic rays by providing a complementary signal to the IceTop Cherenkov tanks. A detailed simulation study of the proposed array was performed to show its capabilities of air-shower detection. An optimisation of the reconstruction was investigated using different lateral particle distribution functions and adjusting the reconstruction parameters. The reconstruction efficiency of the new array as well as its accuracy were evaluated for a chosen configuration.

1. Introduction

The IceTop surface array of the IceCube Observatory measures cosmic rays in the transition region from galactic to extra-galactic sources [1, 2]. The high altitude of the array places the observation level close to the shower maximum enabling more accurate determination of the properties of the primary. However, snow accumulation on the Cherenkov tanks leads to signal attenuation [3, 4] influencing the electron to muon number ratio and thus the cosmic-ray composition analysis. Installing an almost twice as dense array of cost-effective scintillation modules (for a similar total instrumented area) will mitigate this effect. The proposed enhancement foresees the deployment of 37 stations within the IceTop instrumented area, where one station comprises of 7 detectors [5] as illustrated in Fig. 1. This configuration will also improve the veto capability for in-ice neutrino measurements by lowering the detection threshold for cosmic rays.

The difference in response to shower particles between scintillation detectors and Cherenkov tanks requires accurate studies of air-shower characteristics reconstructed by the new detection device. A complete simulation chain combining air-shower cascades and interactions within the detectors has been established to estimate the capabilities of the enhancement and create a preliminary tool for future data analyses.

2. Simulation structure

The final scintillation detector design is under investigation. Two different prototype stations were deployed at the South Pole in the austral summer of 2017/18 for on-site evaluation and testing. The following simulation study is based on a simplified model of the prototype detectors, combining an adequate level of specificity with the possibility to investigate the response of the full planned array to extensive air-showers.
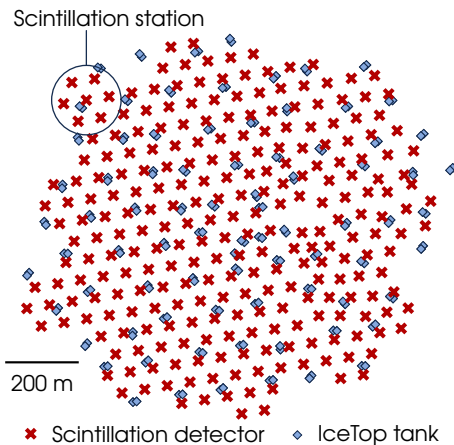
Figure 1. The scheme of the scintillation upgrade. Red crosses show planned positions of scintillation modules and blue squares show positions of IceTop tanks.
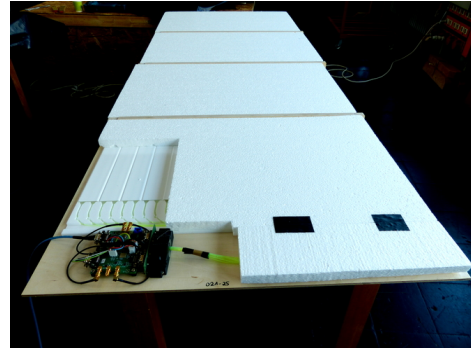

Figure 2. The scintillator bars with out-coming wavelength-shifting fibres and readout system used in one of the prototype stations. The scintillator bars are covered with styrofoam supported by plywood.

2.1. Scintillation detector geometry and definition of signal

The prototype design was inherited from AugerPrime [6]. The scintillation detector consists of 16 polystyrene bars coated with a reflecting TiO_2 layer of 250 μm thickness creating 1.5 m^2 of sensitive area (0.8 m $\times$ 1.875 m). Scintillation photons are guided through the wavelength-shifting fibres to a SiPM-based readout system. To provide light-tightness, the scintillator is wrapped in a polyethylene foil with high static dissipative properties. One of the prototypes is shown in Fig. 2.

The core of the simulations lies in the incorporation of the Geant4 toolkit [7] within the framework of the IceCube standard software. The implemented geometry treats the scintillator bars as the sensitive boxes coated with a reflective layer and placed in an 1 mm aluminium casing, padded with 20 mm plywood support structure and styrofoam. The enclosing details are descriptive of one of the two sets of panels but the differences of the other set of panels are not expected to change the simulations results.

The simulations do not include the fibres and the fibre holes. The output of the detector simulation is the energy deposited within the sensitive material as well as a number of produced scintillation photons calculated by means of Birks' law [8] (assuming a scintillation yield of 11200 photons/MeV and Birks' constant of 0.111 mm/MeV). The simulated signal is defined as the sum of photons generated by all particles crossing the detector and by convention is normalised to the average number of photons generated by vertically passing muons of 3 GeV kinetic energy (VEM = vertical equivalent muon) randomly distributed across the detector. In this case, the reference value used for such normalisation is the peak of the Landau distribution parameterisation [9] fitted to the number of photons (Fig. 3).

2.2. Air-shower simulations

The extensive air-showers are simulated with CORSIKA v7.5600 [10] using Sybill 2.3 [11] (high energy hadronic interaction model) and FLUKA [12] (low energy interaction model). The particles are read out at the observation level of 2838 m (Atmosphere model 13, October 1997 [13]) and further propagated to the scintillation array placed 30 cm lower. The threshold on the secondary particle energy in the air-shower is set to 0.1 GeV for hadrons, 0.1 GeV for muons, 0.3 MeV for electrons and 0.3 MeV for photons. In order to investigate the capabilities
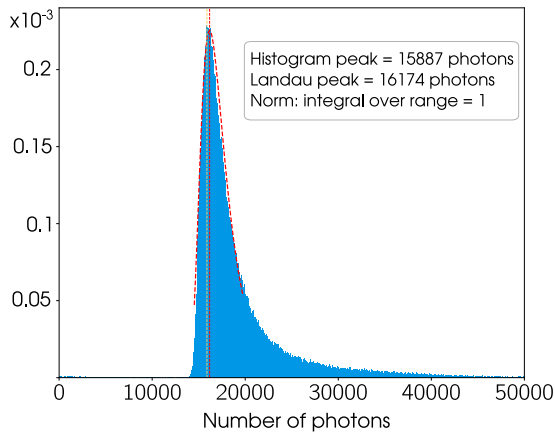
Figure 3. Number of generated photons produced in the scintillation module by 3 GeV vertically muons randomly distributed across the detector. The parametrisation of Landau distribution was taken to estimate the peak value.
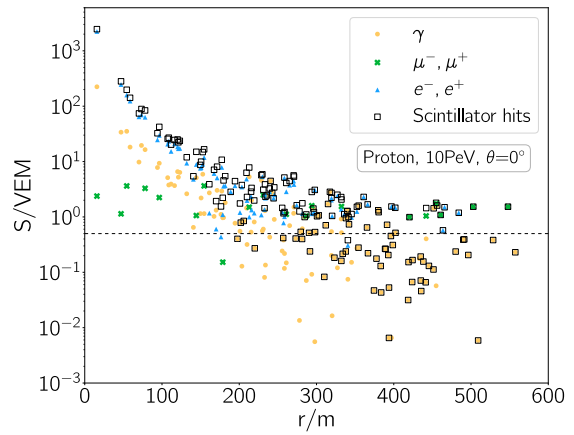
Figure 4. Lateral distribution of air-shower signals. The signals as well as partial contributions from different particle species are shown. The horizontal line indicates the cut (> 0.5 VEM) to be considered in the reconstruction.

of detection in the "knee" region of the cosmic-ray energy spectrum, as well as of primary mass identification, the simulations were conducted for proton and iron primaries of energies 100 TeV–100 PeV with incoming zenith angles from 0° to 40° and azimuth -180° to 180°, and further resampled within the array.

3. Array response

Energy and direction of the primary cosmic ray can be estimated from spatial and temporal distributions of the secondary particle signals which depend on the detector geometry and spacing, as well as on the atmospheric conditions. Therefore the proper description for a given experimental site is essential. Fig. 4 shows an example simulated response of the scintillation array to an air-shower induced by a high-energy proton. The shape of the lateral distribution indicates the size of the shower which is directly connected to the primary energy. The contributions from different particle species indicate the leading signals at different distances to the shower axis. The ratio between the electromagnetic and muonic component reveals the primary particle mass, since heavier primaries generate a higher number of muons.

3.1. Arrival time distributions

The arrival times of the particles hitting each detector allow tracing back the direction of an incoming cosmic ray. This information is included in the curvature function, which represents the signal arrival delay with respect to the plane front assumption. The accuracy of the reconstructed direction is shown in Fig. 6 using two different lateral distribution functions.

3.2. Lateral distributions

The importance of a proper definition of the lateral distribution function and at the same time its challenge lies in the need of simultaneous estimation of core, age and size of the air-shower. Originating from the theoretical Nishimura-Kamata-Greisen description [14, 15], its different modifications (like in [16, 17]) are most frequently used in various experiments like for example Eq. 1 [18]. In addition some groups reported a good agreement of scintillation array results with a function like Eq. 2 accounting for higher scaling with radial distance [19, 20, 21].
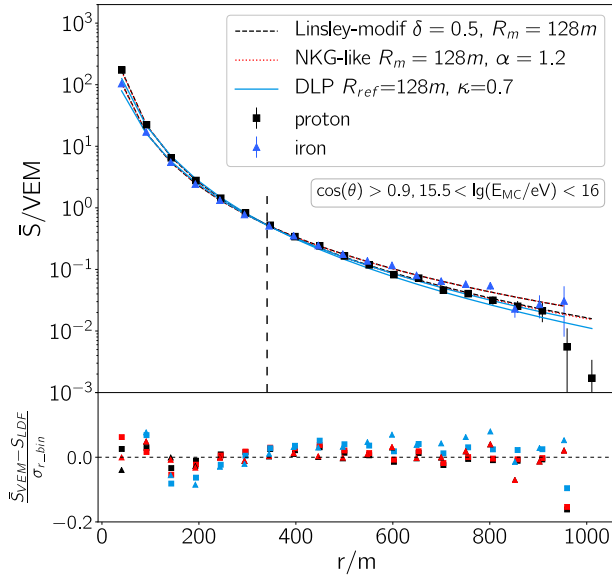
Figure 5. Average lateral distribution of signals for proton (black squares) and iron (blue triangles) primaries with energies $10^{15.5}$–10^{16} eV and arrival directions smaller than $25°$. The crossing region for different primaries is marked with a vertical line. Lines and residual markers represent respectively: black — modified Linsley, blue — NKG-like, red — DLP functions. The fit was obtained with MCMC sampler [23]. The shown parameters are exemplary and R_m refers to the theoretical Molière radius for IceIop atmosphere. Even though average distributions show small deviations from different functions, the stability of single fits vary significantly.

The function used in the standard reconstruction with IceTop tanks is represented by Eq. 3 (in the logarithmic form this equation is called a double logarithmic paraboloid — DLP), which takes into account the flatter shape of the tank response distribution [22].

$$S_{\text{NKG-like}}\left(r\right) = \frac{N}{2\pi R_m^2} \frac{\Gamma(\beta - s)}{\Gamma(s - \alpha + 2)\Gamma(\alpha + \beta - 2s - 2)} \left(\frac{r}{R_m}\right)^{s-\alpha} \left(1 + \frac{r}{R_m}\right)^{s-\beta} \tag{1}$$

$$S_{\text{Linsley}_{\text{modif}}}\left(r\right) = \frac{N}{R_m^2} \left(\frac{r}{R_m}\right)^{-\alpha} \left(1 + \frac{r}{R_m}\right)^{\alpha-\beta} \left[1 + \left(\frac{r}{10R_m}\right)^2\right]^{-\delta} \tag{2}$$

$$S_{\text{DLP}}\left(r\right) = S_{ref}\left(\frac{r}{R_{ref}}\right)^{-\beta - \kappa \log_{10}\left(\frac{r}{R_{ref}}\right)} \tag{3}$$

In the above functions: the parameters α, β, δ, κ and s influence the slope of the function and thus the age of shower development, where R_m and R_{ref} indicate scaling and reference distances. The signal at R_{ref} distance and size of the air-shower, N, correspond to the primary energy.

Fig. 5 shows the average lateral distribution of proton- and iron-induced showers, where the detectors without signals are accounted for. The distance at which two distributions cross is marked. It is important to notice that this point strongly depends on the primary energy and the zenith angle. This distance is of particular interest as it could provide a mass-independent estimate of the primary energy. The choice of proper parameters for a particular function is a challenging task and was evaluated for single air-showers by minimising the negative logarithm of the Poisson likelihood. Based on this the best function was chosen for further reconstruction of individual events.

3.3. Reconstruction performance

The reconstruction performed within the IceTop framework [22, 2] handles the parametrisation of the lateral distribution function and shower-front function in three steps. The distribution of arrival delays with respect to the plane-front is described by the sum of a parabolic and a
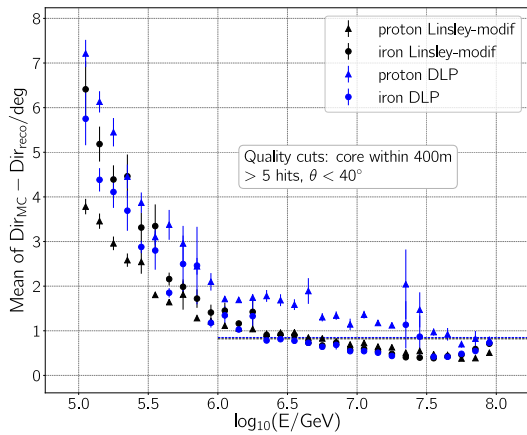
Figure 6. Difference between simulated and reconstructed directions. The blue points correspond to reconstruction with the DLP function and the black ones to the modified Linsley function. The average difference above 1 PeV is smaller than 1° and it is marked in the picture as the horizontal dashed lines for both cases.
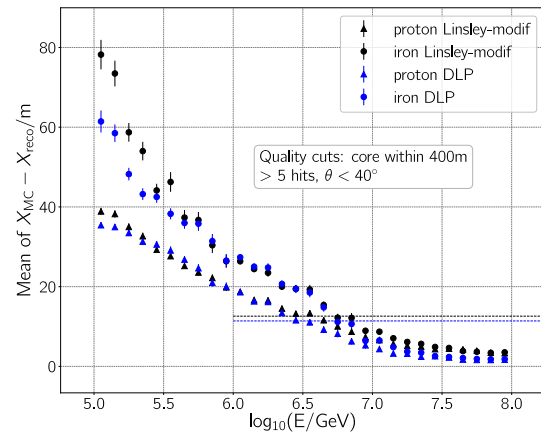
Figure 7. Difference between simulated and reconstructed core positions. The blue points correspond to reconstruction with the DLP function and the black ones to the modified Linsley function. The average difference above 1 PeV is around 12 m and it is marked in the picture as the horizontal dashed lines for both cases.

Gaussian function for a single event. Within the reconstruction the negative log-likelihood is minimised, taking the Poisson distribution for non-zero signals, the Poisson cumulative distribution for silent stations, and a Gaussian distribution for time delays.

The overall reconstruction shown in Fig. 8 was performed using the modified Linsley function with parametrisation on β parameter (the form of parameterisation was adopted from [24, 25]). It shows full efficiency for air-showers even below 1 PeV, which can significantly improve detailed studies of the transition region. The average accuracy of reconstruction above 1 PeV is smaller than 1° in direction (Fig. 6) and around 12 m in core position (Fig. 7). These results are however obtained without refined quality cuts which will improve the accuracy. It is important to note that despite our choice of the function the overall behaviour of reconstruction does not change significantly, but does change across energies.
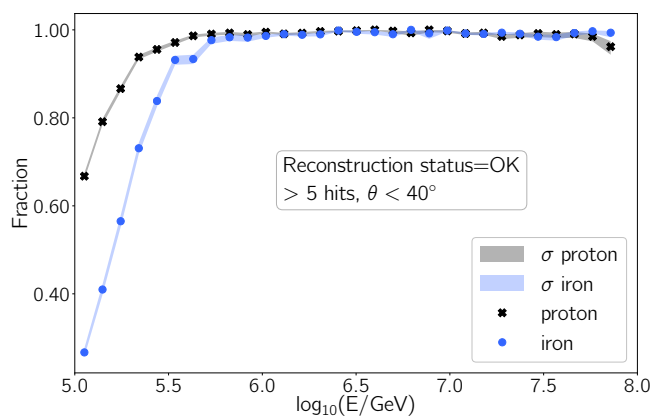

Figure 8. The efficiency of air-shower reconstruction for proton and iron primaries using the modified Linsley function. The proposed array can reconstruct air showers with full efficiency even below 1 PeV. At lower energies the reconstruction will improve the veto efficiency for in-ice measurements. Sigma is defined as the Wald interval [26].

4. Concluding remarks

The scintillation enhancement of the IceTop array was investigated using a full simulation framework. The fundamental distributions and array response to the air-showers were obtained together with studies of lateral distribution functions. After adjusting the existing reconstruction routine, the efficiency of air-shower reconstruction has shown a possibility to lower the measured energy threshold, going below the "knee" region. The results qualitatively indicate the upgrade's capabilities and reveal its challenges for future combined analyses of scintillation and the Cherenkov signals.

Specifics of the new array require further detailed studies, especially in order to account for different behaviours of fluctuations and therefore the proper choice of a likelihood function for the minimisation procedure. Further studies and improvements are ongoing, including an evaluation of the validity of the functions employed in order to obtain a more reliable estimate of the primary energy.

References

[1] Abbasi R *et al* (IceCube Collaboration) 2013 *Nucl. Instrum. Meth. A* **700** 188-220 [arXiv:1207.6326]
[2] Abbasi R *et al* (IceCube Collaboration) 2013 *Astropart. Phys.* **44** 40-58 [arXiv:1202.3039]
[3] Rawlins K *et al* (IceCube Collaboration) 2013 *PoS(ICRC2013)* 1106 37-40 [arXiv:1309.7006]
[4] Rawlins K *et al* (IceCube Collaboration) 2015 *PoS(ICRC2015)* 0628 68-75 [arXiv:1510.05225]
[5] Huber T *et al* (IceCube-Gen2 Collaboration) *PoS(ICRC2017)* 401 62-68 [arXiv:1710.01207]
[6] Aab A *et al* (Pierre Auger Collaboration) 2016 The Pierre Auger Observatory Upgrade - Preliminary Design Report [arXiv:1604.03637]
[7] Agostinelli S *et al* (GEANT4 Collaboration) 2003 *Nucl. Instrum. Meth. A* **506** 250-303
[8] Birks J B 1951 *Proc. Phys. Soc. A* **64** 874-877
[9] Moyal J E 1955 *Phil. Mag.* **46** 263-280
[10] Heck D *et al* 1998 Report FZKA 6019 [`https://publikationen.bibliothek.kit.edu/270043064`]
[11] Riehn F *et al* 2015 A new version of the event generator Sibyll *PoS(ICRC2015)* 558 [`inspirehep.net/record/1395980/files/ICRC2015_558.pdf`]
[12] Ferrari A *et al* 2005 *FLUKA: A Multi-Particle Transport Code* CERN-2005-10, INFN/TC_05/11, SLAC-R-773
[13] `https://ccmc.gsfc.nasa.gov/modelweb/models/msis_vitmo.php`
[14] Greisen K 1956 *Progress in Cosmic Ray Physics* vol 3 ed. by Wilson J G and Robinson G (Amsterdam: North Holland Publ.Co.) chapter 1 pp 19-37
[15] Kamata K and Nishimura J 1958 *Prog. Theor. Phys. Suppl.* **6** 93-155
[16] Linsley J 1962 *J. Phys. Jpn. Suppl. A-III* **17** 148
[17] Capdeviellev J N and Cohen F 2005 *J. Phys. G: Nucl. Part. Phys.* **31** 507-524
[18] Apel W D *et al* (KASCADE Collaboration) 2006 *Astropart. Phys.* **24** 467-483 [arXiv:astro-ph/0510810]
[19] Lagutin A A and Raikin R I 2001 *Nucl. Phys. B (Proc. Suppl.)* **97** 13
[20] Lagutin A A, Raikin R I, Inoue N and Misaki A 2002 *J. Phys. G: Nucl. Part. Phys.* **28** 1259-1274
[21] Yoshida S 1995 *J. Phys. G: Nucl. Part. Phys.* **20** 651-665
[22] Klepser S 2008 Reconstruction of Extensive Air Showers and Measurement of the Cosmic Ray Energy Spectrum in the Range of 1-80PeV at the South Pole. PhD thesis, Humboldt-Universitt zu Berlin
[23] Foreman-Mackey D *et al* 2013 *Publ. Astron. Soc. Pac.* **125** 306-312 [arXiv:1202.3665]
[24] Grieder P K F 2010 *Extensive Air Showers: High Energy Phenomena and Astrophysical Aspects — A Tutorial, Reference Manual and Data Book* (Springer-Verlag Berlin Heidelberg) chapter 8 pp 390-391
[25] Glushkov A V, Makarov A K and Makarov I T 2011 *Proceedings 32nd International Cosmic Ray Conference (ICRC 2011)* **6** 153-155
[26] Brown L D *et al* 2001 *Statist. Sci.* **16** (2) 101-133